

EXCAVATOR DYNAMICS AND EFFECT OF SOIL ON DIGGING

P. K. Vähä

Technical Research Centre of Finland
 Electronics Laboratory
 P.O. Box 200, Oulu, Finland

A. J. Koivo

School of Electrical Engineering
 Purdue University

M. J. Skibniewski

School of Civil Engineering
 Purdue University
 West Lafayette, Indiana 47907

Keywords: Excavator dynamic model, soil model

ABSTRACT

Automation of excavation work calls for a robotic system able to perform the planned digging work, and responsive to interaction forces experienced during excavation. The development of automated excavation control method requires a dynamic model to describe the evolution of the excavator motion with time. The joint torques of the boom mechanism are generated by hydraulic rams which also affect the torques at other joints. A Newton-Euler formulation is applied to derive a dynamic model for an excavator in this paper. Secondly, for determining the soil resistance the effect of soil on digging is described. Combining these equations makes it possible to design a control method for an excavator.

1. INTRODUCTION

Automation of excavation work poses a requirement for a robotic system able to perform the planned digging work and responsive to interaction forces experienced during excavation. For that purpose a complete dynamic model is required. This paper presents the dynamic model for an excavator and the effect of type of soil on digging. The dynamic model of a manipulator based on Newton-Euler equations of motion specifies the equations of motion relative to a chosen coordinate system. The equations of motion can be obtained by forming Euler-Lagrange's equation on the basis of Lagrange energy function, or by considering each link as a free body and obtaining the equations of motion for each link in succession on the basis of Newton's and Euler's laws.

The application of Lagrange's formulation gives the designer a physical insight needed to understand the behavior of the overall system, but the formulation is computationally complex. Using Newton's and Euler's equations each link in succession is isolated as a free body, resulting in a recursive model for a link involving variables of the adjacent links. Since the joint torques of the boom mechanism are generated by hydraulic rams which also affect the torques at other joints, the method can be applied in a straight-forward manner. The equations describe in detail the translational and rotational dynamics of the link, containing internal forces and torques.

Newton-Euler equations of motion for each link of a serial link manipulator can be expressed either in Cartesian base or local coordinate frames. Since the mass moment of inertia depends on the configuration of the manipulator the equations of motion for each link are expressed in a local

coordinate frame moving with the link. Then the mass moment of inertia in the moving coordinate frame remains constant during the motion.

In digging the soil resists bucket movements, demanding the excavator to comply with the restrictions imposed by the environment. An essential variable in compliant motion is the generalized force exerted by the end-effector or the bucket of an excavator. The contact between the bucket and the soil is soft, since the bucket penetrates into the soil (Vähä 1990). In order to study the control of an excavator during digging, the interfacing contact of the bucket with the soil must also be considered. The task of the excavator is to scoop soil according to a preplanned digging trajectory despite of varying soil resistance. If, however, the soil resistance is so high that the excavator is not able to follow the preplanned trajectory, it should have an ability to change its scooping path on line by reducing digging depth and taking less soil into the bucket.

2. KINEMATICS

In order to describe the position of the points on the mechanism of an excavator, coordinate systems are first defined. A fixed Cartesian (rectangular and right-hand) coordinate system is assigned to body of the excavator. The local coordinate frames are assigned to each link of the mechanism. A systematic method to define the local coordinate systems for the serially connected links (upperstructure, boom, arm and bucket) of the excavator is accomplished by applying Denavit and Hartenberg procedure (Koivo 1989). The resulting coordinate frames for the links of the excavator are shown in Fig. 1. It should be noticed that the first link rotates on the supporting base about the vertical axis. The rotational axes for the other joints are horizontal.

For determining the transformation matrices, structural kinematic parameters are defined and presented in Table 1, where d_i , a_i , α_i and θ_i are structural kinematic parameters of the Denavit Hartenberg procedure.

Table 1.	link (1)	d_i (2)	a_i (3)	α_i (4)	θ_i (5)
Structural kinematic parameters	1	0	a_1	90	θ_1
	2	0	a_2	0	θ_2
	3	0	a_3	0	θ_3
	4	0	a_4	0	θ_4

The transformation matrices for rotational joints assume the following general form:

$$A_{i-1}^i = \begin{vmatrix} \cos \theta_i & -\cos \alpha_i \sin \theta_i & \sin \alpha_i \sin \theta_i & a_i \cos \theta_i \\ \sin \theta_i & \cos \alpha_i \cos \theta_i & -\sin \alpha_i \cos \theta_i & a_i \sin \theta_i \\ 0 & \sin \theta_i & \cos \alpha_i & d_i \\ 0 & 0 & 0 & 1 \end{vmatrix} \quad (1)$$

3. NEWTON-EULER FORMULATION

By applying the algorithm of Newton-Euler's formulation the equations of motion can be obtained (Goldstein 1980, Koivo 1989). The rotation submatrices can be obtained first from the homogeneous transformation matrices, and the inverse of rotation matrix is equal to its transpose.

First, the forward difference equations are determined for each of the joints. Following the recursive relationship for positions, velocities and accelerations in local coordinate frames of links and centroids of the links

can be determined, as well as the external forces and moments acting on each link.

In the local coordinate frame the joint can rotate only about the z_i -axis when the inertia takes the following form:

$$I_{0i} = \begin{vmatrix} \frac{1}{2}I_{zi} & 0 & 0 \\ 0 & \frac{1}{2}I_{zi} & 0 \\ 0 & 0 & -\frac{1}{2}I_{zi} \end{vmatrix} \quad (2)$$

where I_{0i} is a symmetric matrix and I_{zi} is the moment of inertia about the axis of rotation, z-axis. The second mass moments are defined as follows:

$$I_{zi} = \int (P_{xi}^2 + P_{yi}^2) dm \quad (3)$$

The integration is over the mass of the link "m". The term I_{zi} is the second mass moment of inertia about the axis indicated with a letter.

The mass moment of inertia for the upperstructure can be calculated by adding mass moments of separate parts. The moment can be calculated by applying the mass moment of inertia of the rectangular about centroidal axial axis, and then using the parallel axis theorem to obtain it about the center of gyration. The inertia of the boom can also be calculated in stages. The boom shape can be approximated by the use of triangles. The total inertia is then achieved by summing up the inertias of these triangles. The mass inertia of the arm can be obtained by using the same principle as in the boom case, e.g. dividing the arm into two triangles and calculating their moments separately and summing them up. The inertia of the bucket is calculated in three phases; the walls are approximated to be semicircles and the bottom to be a semiannulus (Pilkey and Pilkey 1974).

Once the velocities and accelerations for the links and their gravity centers have been obtained recursively for each link, then the backward difference equations can be determined by using general formulas (Koivo 1989).

The force torque relations for the links are written according to the following method. The required force and torque at joint 4 ($i = 4$) can be calculated in a straightforward manner (Koivo 1989). In calculations of the moments for the third and second joints the forces and moments generated by the driving cylinders of the forth and third joints must also be considered. The force of the driving cylinder 4 generates a moment, which must be added to the total moment of joint 3. The moment arm l_{c4y} from ram 4 to joint 3 is taken as a constant, because its variation with θ_4 is negligible. Correspondingly, the ram force 3 has to be considered in calculations of moments at other joints.

As an example, the dynamic model for an excavator is presented in the digging mode, which means that the rotation angle θ_1 is held constant during that time. Now it can be assumed that the movements of the excavator mechanism during digging take place in the plane parallel to the mechanism. Thus, the model takes the following form:

$$\begin{vmatrix} T_2 \\ T_3 \\ T_4 \end{vmatrix} = \begin{vmatrix} d_{21} & d_{22} & d_{23} \\ d_{31} & d_{32} & d_{33} \\ d_{41} & d_{42} & d_{43} \end{vmatrix} \cdot \begin{vmatrix} \ddot{\theta}_2 \\ \ddot{\theta}_3 \\ \ddot{\theta}_4 \end{vmatrix} + \begin{vmatrix} h_2 \\ h_3 \\ h_4 \end{vmatrix} + \begin{vmatrix} g_2 \\ g_3 \\ g_4 \end{vmatrix} + \begin{vmatrix} f_{c2} \\ f_{c3} \\ f_{c4} \end{vmatrix} \quad (4)$$

where

$$d_{21} = (4a_2^1 4g^m 4c_{347} + 4a_3^1 4g^m 4c_{47} + 4a_2^1 3g^m 3c_{36} + 4a_2 a_3^m 4c_3 + 21 4g^2 m_4 + 2a_3^2 m_4 + 2a_2^2 m_4 + 21 3g^2 m_3 + 2a_2^2 m_3 + 21 2g^2 m_2 + I_{z4} + I_{z3} + I_{z2})/2 \quad (5)$$

$$d_{22} = (2a_2^1 4g^m 4c_{347} + 4a_3^1 4g^m 4c_{47} + 2a_2^1 3g^m 3c_{36} + 2a_2 a_3^m 4c_3 + 21 4g^2 m_4 + 2a_3^2 m_4 + 21 3g^2 m_3 + I_{z4} + I_{z3})/2 \quad (6)$$

$$d_{23} = (2a_2^1 4g^m 4c_{347} + 2a_3^1 4g^m 4c_{47} + 21 4g^2 m_4 + I_{z4})/2 \quad (7)$$

$$d_{31} = (2a_2^1 4g^m 4c_{347} + 4a_3^1 4g^m 4c_{47} + 2a_2^1 3g^m 3c_{36} + 2a_2 a_3^m 4c_3 + 21 4g^2 m_4 + 2a_3^2 m_4 + 21 3g^2 m_3 + I_{z4} + I_{z3})/2 \quad (8)$$

$$d_{32} = (4a_3^1 4g^m 4c_{47} + 21 4g^2 m_4 + 2a_3^2 m_4 + 21 3g^2 m_3 + I_{z4} + I_{z3})/2 \quad (9)$$

$$d_{33} = (2a_3^1 4g^m 4c_{47} + 21 4g^2 m_4 + I_{z4})/2 \quad (10)$$

$$d_{41} = (2a_2^1 4g^m 4c_{347} + 2a_3^1 4g^m 4c_{47} + 21 4g^2 m_4 + I_{z4})/2 \quad (11)$$

$$d_{42} = (2a_3^1 4g^m 4c_{47} + 21 4g^2 m_4 + I_{z4})/2 \quad (12)$$

$$d_{43} = (21 4g^2 m_4 + I_{z4})/2 \quad (13)$$

$$h_2 = -(a_2^1 4g^m 4s_{347} + a_3^1 4g^m 4s_{47})(\dot{\theta}_2 + \dot{\theta}_3 + \dot{\theta}_4)^2 + (a_3^1 4g^m 4s_{7-4} - a_2^1 3g^m 3s_{36} - a_2 a_3^m 4s_{34} - 2a_3^2 m_4 c_{4s_4}) \cdot (\dot{\theta}_2 + \dot{\theta}_3)^2 + (a_2^1 4g^m 4s_{347} + a_2^1 3g^m 3s_{36} + a_2 a_3^m 4s_3) \cdot \dot{\theta}_2^2 + b_2 \dot{\theta}_2 \quad (14)$$

$$h_3 = -(a_3^1 4g^m 4s_{47})(\dot{\theta}_2 + \dot{\theta}_3 + \dot{\theta}_4)^2 + (a_3^1 4g^m 4s_{7-4} - 2a_3^2 m_4 c_{4s_4}) \cdot (\dot{\theta}_2 + \dot{\theta}_3)^2 + (a_2^1 4g^m 4s_{347} + a_2^1 3g^m 3s_{35} + a_2 a_3^m 4s_3) \cdot \dot{\theta}_2^2 + b_3 \dot{\theta}_3 \quad (15)$$

$$h_4 = (a_3^1 4g^m 4s_{7-4})(\dot{\theta}_2 + \dot{\theta}_3)^2 + a_2^1 4g^m 4s_{237} \dot{\theta}_2^2 + b_4 \dot{\theta}_4 \quad (16)$$

$$g_2 = g^1 4g^m 4c_{2347} + g^1 3g^m 3c_{236} + g^1 2g^m 2c_{25} + g a_3^m 4c_{23} + g a_2^m 4c_2 + g a_2^m 3c_2 \quad (17)$$

$$g_3 = g^1_{4g} m_4 c_{2347} + g^1_{3g} m_3 c_{236} + g a_3 m_4 c_{23} \quad (18)$$

$$g_4 = g^1_{4g} m_4 c_{2347} \quad (19)$$

$$f_{c2} = l_{c4y} F_{4c} + l_{c3y} F_{3c}, \quad f_{c3} = l_{c4y} F_{4c}, \quad f_{c4} = 0 \quad (20)$$

In order to make the excavator bucket to move along the desired preplanned trajectory, the restrictions of the soil have to be incorporated into the excavator dynamic model. Thus, the total manipulator dynamics can be presented in a general form:

$$D(\theta)\ddot{\theta} + H(\dot{\theta}, \theta) + G(\theta) + F_c(\theta) = F - J(\theta)' F_e \quad (21)$$

where matrix $J'(\theta)$ signifies the transpose of Jacobian matrix evaluated at $\theta = \theta(t)$. The Jacobian matrix for the excavator shown in Figure 1, when the digging plane is along x-axis, can be presented as follows:

$$J(\theta)' = \begin{vmatrix} a_4 \cdot s_{234} + a_3 \cdot s_{23} + a_2 \cdot s_2 & -a_4 \cdot c_{234} - a_3 \cdot c_{23} - a_2 \cdot c_2 & 1 \\ a_4 \cdot s_{234} + a_3 \cdot s_{23} & -a_4 \cdot c_{234} - a_3 \cdot c_{23} & 1 \\ a_4 \cdot s_{234} & -a_4 \cdot c_{234} & 1 \end{vmatrix} \quad (22)$$

and the generalized force is:

$$F_e = \begin{vmatrix} f \\ f_{ex} \\ f_{ez} \\ m_{ey} \end{vmatrix} \quad (23)$$

since $f_{ey} \equiv 0$, $m_{ex} \equiv 0$, $m_{ez} \equiv 0$

4. CALCULATION OF REQUIRED RAM FORCES

The driving forces at joints 2, 3 and 4 are generated by their driving cylinders. Therefore the torques determined above have to be transformed to their corresponding ram forces, Fig. 2. This requires the calculation of lengths for lever arms as a function of joint angles (appendices I and II). According to the equations, the torque at joint 4 is calculated first and transformed to a corresponding ram force. Then the torque at joint 3 can be calculated by substituting it to the torque equation of joint 3. The torque at joint 2 is also a function of the ram forces at joints 4 and 3 which have to be substituted into that equation.

5. EFFECT OF TYPE OF SOIL ON DIGGING

The soil resists the penetration of the bucket and scooping of a bucketful of soil demands varying amount of energy depending on the type of soil, area of the cutting edge of the bucket blades and thickness of the cut, Fig. 3. The maximum cutting ability of the bucket is consistent with the direction of the cutting blades. During the digging of soil by excavator there are three tangential resistances resisting the movement of the bucket (see Alekseeva et al. 1985):

$$\bar{P}_t = \bar{P}_p + \bar{P}_m + \bar{P}_g \quad (24)$$

where

- \bar{P}_p soil resistance to cutting
 \bar{P}_m frictional resistance of the working tool with the ground
 \bar{P}_g resistance to movement of the prism of soil, and soil movement in the bucket

The tangential resistance expressed in a more specific form is:

$$\bar{P}_t = k_s b h + \mu N + \varepsilon (1 + q_n) q k_n \quad (25)$$

where

- k specific resistance to cutting, N/m^2
 b, h width and thickness of the cut slice of the soil, respectively, m
 μ coefficient of friction of the bucket with the ground
 N pressure force of the bucket on the soil, N
 q_n volume of the prism of soil expressed as a fraction of the volume of the bucket
 q volume of the bucket
 ε coefficient of resistance to filling of the bucket and movement of the prism of soil, N/m^2 , $\approx 0.1 \cdot k_s$
 k_n coefficient of filling the bucket; the ratio of the volume of ripped soil in the bucket to the geometric volume of the bucket.

The resultant resistance force to digging is at certain angle to the bucket trajectory and varies depending on the digging angle and the wear and tear of the cutting edge. The normal component is calculated as a function of the tangential component as follows:

$$\bar{P}_n = \beta \bar{P}_t, \quad 0.1 \leq \beta \leq 0.45 \quad (26)$$

For simulating the behavior of the excavator dynamics during digging the former equations can be used. A small cutting angle between the bucket bottom and the digging direction should be maintained to achieve the resultant force parallel to the digging direction, Fig. 3. The equations (25) and (26) account for the interaction forces experienced when the bucket penetrates into the soil to get a scoopful of soil. In a subsequent computer study conducted at Purdue that coefficient was held constant ($\beta = 0.1$). This corresponds to a deviation of 5.7° . Then the horizontal and vertical digging resistances get the following equations:

$$P_h = k_p (k_s b h + \mu N + \varepsilon \cdot (1 + V_s/V_b) \cdot b \cdot \sum(h\delta x)) \cos(\theta_d - 0.1) \quad (27)$$

$$P_v = k_p (k_s b h + \mu N + \varepsilon \cdot (1 + V_s/V_b) \cdot b \cdot \sum(h\delta x)) \sin(\theta_d - 0.1) \quad (28)$$

where

- k = 1.005
 θ^p = digging (penetration) angle;
 V^d = volume of the prism of soil;
 V^s = volume of the bucket
 $\sum^b(h\delta x)$ = amount of soil ripped into bucket

These forces are then applied in the dynamic model of an excavator. The resistance to movement of the prism of soil, and the soil movement in the bucket has the least influence on the digging force being less than 10%. From the above knowledge the coefficients needed for calculating the digging

force can be evaluated.

6. CONCLUSIONS

The dynamic model of an excavator presented above provides a useful computational platform for investigating the machine behavior of a typical excavator. In particular, the model can serve as a basis for computer simulation of excavator behavior during gross motion and digging of soil by excavator bucket. Moreover, it is useful in designing a controller to make the excavator motion track a specified path for a given digging task.

References

- Alekseeva, T.V., Artem'ev, K.A., Bromberg, A.A., Voitsekhovskii, R.I., Ul'yanov, N. A. (1985). *Machines for Earthmoving Work, Theory and Calculations*. Mashinostroenie Publishers, Moscow, 1072. Amerind Publishing Co. Pvt. Ltd., New Delhi (Translated from Russian).
- Seward, D., Bradley, D., Bracewell, R. (1988). "The development of research models for automatic excavation." *Proceedings of the 5th International Symposium on Robotics in Construction*, Tokyo, Japan, pp. 703 - 708.
- Goldstein, H. (1980). *Classical Mechanics*, Addison-Wesley, Reading, MA.
- Koivo, A. J. (1989). *Fundamentals for control of robotic manipulators*. John Wiley & Sons, Inc., New York, N.Y.
- Luh, J.Y.S, Walker, M.W. Paul, R.P.C. (1980). "On-line computational scheme for mechanical manipulators." *Journal of Dynamic Systems, Measurement, and Control*, Transactions of the ASME, 102(6), pp. 120-127.
- Pilkey, W.D., Pilkey, O.H. (1974). *Mechanics of Solids*. Quantum Publishers, Inc., New York, N.Y.
- Vähä, P.K. (1990). "Modelling and control of cognitive excavation." *Technical Report*, School of Civil Engineering, Purdue University, West Lafayette, IN.

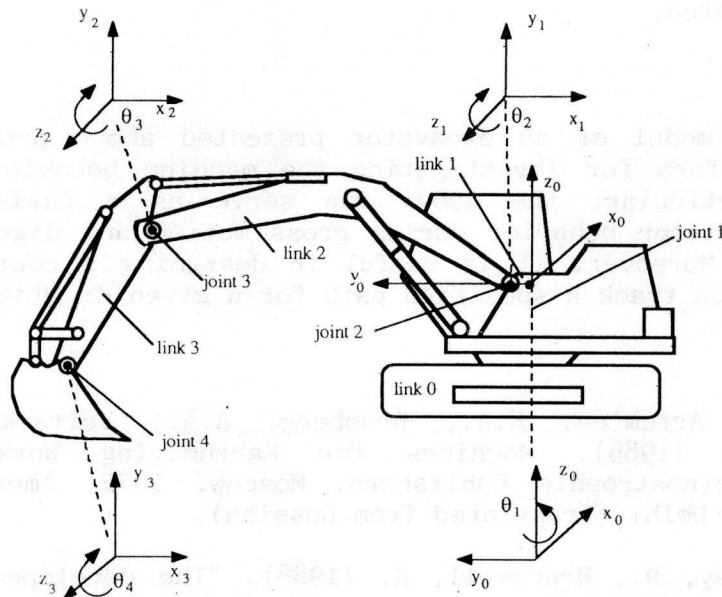


Figure 1. Typical excavator and its coordinate frames.

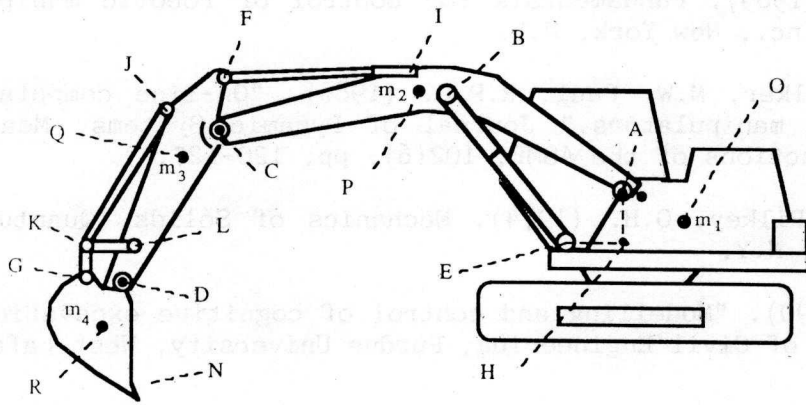
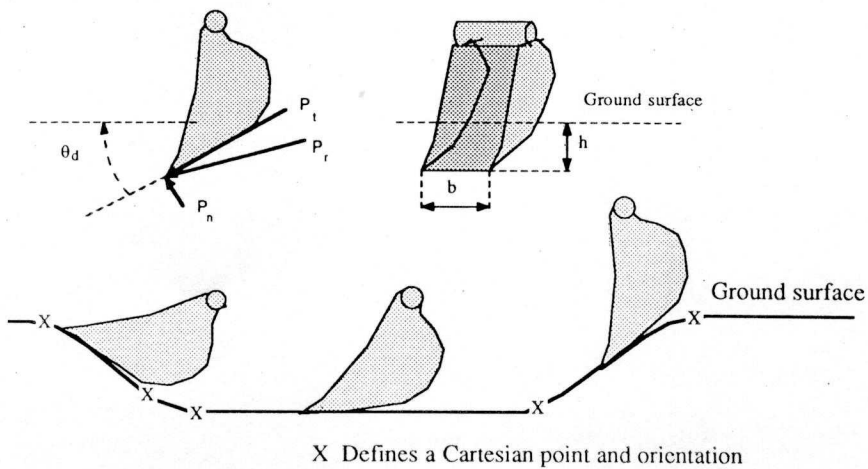


Figure 2. Excavator geometry.



X Defines a Cartesian point and orientation

Figure 3. Schematics of excavation path geometry.

APPENDIX I - Calculation of Required Ram Forces

The lever arm and force at joint 2 are:

$$l_{m2} = \frac{l_{ab} \cdot c_{28} \cdot (l_{ab} \cdot s_{28} + l_{ah})}{[(l_{ab} \cdot c_{28} - l_{he})^2 + (l_{ab} \cdot s_{28} + l_{ah})^2]^{\frac{1}{2}}} \quad (1)$$

$$F_{2c} = T_2 / l_{m2} \quad s_{28} = \sin(\theta_2 + \theta_8) \quad (2)$$

Correspondingly, the force and the lever arm at joint 3 are:

$$F_{c3} = T_3 / l_{m2}, \quad l_{m2} = l_{ci} (1 - e^2)^{\frac{1}{2}} \quad (3)$$

$$e = \frac{2l_{ci}^2 - 2l_{cf} \cdot l_{ci} \cdot c_{39}}{2l_{ci}[-2l_{cf} \cdot l_{ci} \cdot c_{39} + l_{ci}^2 + l_{cf}^2]^{\frac{1}{2}}} \quad (4)$$

$$c_{39} = \cos(\theta_3 + \theta_9) \quad (5)$$

Finally, the length of the lever arm at joint 4 is:

$$F_{c4} = T_4 / l_{m4} \quad l_{m4} = -l_{dg} \cdot \cos(\theta_{19} + \theta_{14}) \cdot \sin(\theta_4 - \alpha) \quad (6)$$

$$\alpha = \theta_{16} + \theta_{15} + \theta_{14} + \theta_{10} \quad (7)$$

$$\theta_{14} = \cos^{-1} \left(\frac{2l_{dl} \cdot l_{dg} \cdot \cos(\theta_4 - \theta_{10}) + l_{kg}^2 + l_{kl}^2 - l_{dm}^2 - l_{dl}^2}{2l_{kl} \cdot l_{kg}} \right) \quad (8)$$

$$\theta_{15} = \cos^{-1} \left(\frac{-2l_{gl} \cdot l_{dg} \cdot \cos(\theta_4 - \theta_{10}) + l_{kl}^2 + l_{dl}^2}{2l_{kl} \cdot l_{kg}} \right) \quad (9)$$

$$\theta_{16} = \cos^{-1} \frac{2l_{dl}^2 - 2l_{dl} \cdot l_{dg} \cdot \cos(\theta_4 - \theta_{10}) c_{410}}{2l_{dl}(-2l_{dl} \cdot l_{dg} \cdot c_{410} + l_{dg}^2 + l_{dl}^2)^{\frac{1}{2}}} \quad (10)$$

$$\theta_{19} = \cos^{-1} \left(\frac{2l_{kl}^2 - 2l_{jl} \cdot l_{kl} \cdot \cos(\theta_{16} + \theta_{15} + \theta_{11})}{2l_{kl}(-2l_{jl} \cdot l_{kl} \cdot \cos(\theta_{16} + \theta_{15} + \theta_{11}) + l_{kl}^2 + l_{jl}^2)^{\frac{1}{2}}} \right) \quad (11)$$

APPENDIX II - List of Symbols

Lengths of links

$$\begin{aligned} a_1 &= 0.05 \text{ m} \\ a_2 &= 5.16 \text{ m} \\ a_3 &= 2.59 \text{ m} \\ a_4 &= 1.33 \text{ m} \end{aligned}$$

Mass centers

$$\begin{aligned} l_{1g} &= 0.61 \text{ m} & l_{3g} &= 0.64 \text{ m} \\ l_{1gz} &= 0.21 \text{ m} & l_{4g} &= 0.65 \text{ m} \\ l_{2g} &= 2.71 \text{ m} & & \end{aligned}$$

$$\begin{aligned} \theta_5 &= \text{angle between lines AP and AC (0.2566 rad)} \\ \theta_6 &= \text{angle between lines CD and CQ (0.3316 rad)} \\ \theta_7 &= \text{angle between lines DR and DN (0.3944 rad)} \\ \theta_8 &= \text{angle between lines AB and AC (0.4957 rad)} \\ \theta_9 &= \pi - \theta_{91} - \theta_{92} \\ \theta_{91} &= \text{angle between lines CD and CF (2.71049 rad)} \\ \theta_{92} &= \text{angle between lines CA and CI (0.47822 rad)} \\ \theta_{10} &= \pi - \theta_{101} - \theta_{102} \\ \theta_{101} &= \text{angle between lines DN and DG (2.19737)} \\ \theta_{102} &= \text{angle between lines CL and CD (0.15359)} \\ \theta_{11} &= \text{angle between lines JL and LD (0.13265)} \end{aligned}$$

Masses of links

$$\begin{aligned} m_1 &= 6420 \text{ kg} & m_3 &= 735 \text{ kg} \\ m_2 &= 1566 \text{ kg} & m_4 &= 432 \text{ kg} \end{aligned}$$

Inertial moments

$$\begin{aligned} I_{z1} &= 11748.6 \text{ kg m}^2 & I_{z3} &= 727.7 \text{ kg m}^2 \\ I_{z2} &= 14250.6 \text{ kg m}^2 & I_{z4} &= 224.6 \text{ kg m}^2 \end{aligned}$$

Length between points I and J is denoted as l_{ij} , i.e.:

$$\begin{aligned} l_{ab} &= 2.31 \text{ m} & l_{jl} &= 1.93 \text{ m} & l_{he} &= 0.42 \text{ m} & l_{g1} &= 0.40 \text{ m} \\ l_{ah} &= 0.56 \text{ m} & l_{kl} &= 0.50 \text{ m} & l_{cf} &= 0.77 \text{ m} & l_{gm} &= 0.40 \text{ m} \\ l_{ci} &= 2.80 \text{ m} & l_{km} &= 0.50 \text{ m} & l_{3cy} &= 1.37 \text{ m} & l_{4cy} &= 0.63 \text{ m} \end{aligned}$$

l_{3cy} and l_{4cy} are the tangential distances from points I and J to lines AC and CD, respectively.

$$g = -9.87 \text{ m/s}^2$$